ELSEVIER

Journal of Power Sources 90 (2000) 70–75

JOURNAL OF POWER SOURCES

www.elsevier.com/locate/jpowsour

Dispersion of Sn and SnO on carbon anodes

Jim Yang Lee [a,*], Ruifen Zhang [a], Zhaolin Liu [b]

[a] *Department of Chemical and Environmental Engineering, National University of Singapore, 10 Kent Ridge Crescent, 119260, Singapore*
[b] *Institute of Materials Research and Engineering, 10 Kent Ridge Crescent 119260, Singapore*

Received 14 November 1999; received in revised form 5 February 2000; accepted 15 February 2000

Abstract

Sn and SnO were supported on large surface-area synthetic graphite (KS6) to obtain composite materials with improved electrochemical performance relative to bulk Sn and SnO. In general the composites are superior to the mechanical mixtures of KS6 and Sn (or SnO) of similar overall compositions in many performance areas. The Sn–KS6 composites increase the reversible capacity of graphite at some expense of the cyclability. It was observed that Sn could also contribute to the irreversible capacity loss in the first cycle, probably through a mechanism similar to solid electrolyte interface (SEI) formation on carbonaceous surfaces. The KS6–SnO composites have good reversible capacities, rate capability and cycle life, although their irreversible capacity losses in the first cycles are necessarily higher because of the requisite electro-reduction reaction to convert the oxide precursor into Sn-based Li storage compounds. The observation of specific capacities that are larger than the weighted sums of the capacities of SnO and graphite suggests the presence of synergistic interaction between the two constituents.

Keywords: Sn dispersion; SnO dispersion; Carbon anodes

1. Introduction

Sn-based Li storage materials have once been considered as the most promising replacement of carbonaceous anodes in lithium ion batteries. The rise to prominence owes a large part to the publicity generated from Fujifilm's announcement [1], and the numerous scientific investigations that follow thereafter (e.g. Refs. [2–9]). The high capacity on both a gravimetric and volumetric basis and the low potential of Li ion intercalation are all very desirable material properties. There is, however, a large volume expansion and contraction problem associated with Li^+ insertion and removal reactions, respectively. The internal stresses arising from the volume changes would eventually lead to material failure by mechanical disintegration, and poor cycling performance in applications. It has been suggested that reducing the particle size of the Li^+ storage material may improve the situation [9], although some preliminary theoretical calculations appear to indicate otherwise [10,11]. We envision that the utilisation of the Li^+ storage material is not compromised even if the material is fragmented into smaller particles provided that the latter can remain mechanically and electrically connected. The unusually good cyclability of tin composite oxide (TCO) anodes relative to Sn and Sn alloys can be attributed to the presence of Sn as finely divided particles in a network of Li_2O (formed upon the first charge) and glass formation promoters that hinders the aggregation of Sn particles. In this work, Sn-based Li ion storage materials are dispersed in synthetic graphite hosts, which provide not only mechanical and conductivity support for the dispersed phase, but are also by themselves electrochemically active towards Li^+ insertion and removal. If the preparation can be optimised, this implementation should provide improvements over material designs that are based on the use of one or more inactive phases to restrain the pulverisation of the Li–Sn alloy system during charge and discharge reactions [4].

2. Experimental

2.1. Materials preparations

2.1.1. Dispersion of Sn on synthetic graphite KS6

Synthetic graphite KS6 (TimCal, BET surface area = 19 m^2/g) was suspended in an acidified (pH = 3) $SnCl_2$

* Corresponding author. Tel.: +65-874-2899; fax: +65-779-1936.
E-mail address: cheleejv@nus.edu.sg (J.Y. Lee).

0378-7753/00/$ - see front matter
PII: S0378-7753(00)00450-X

solution (0.06 M $SnCl_2$ in 0.01 M HCl) to which a 0.15 M $NaBH_4$ solution was subsequently added with continuous stirring to precipitate Sn^{2+} as elemental Sn. At the completion of the reaction, the solid phase was removed by filtration followed by copious washing with distilled water and drying in a vacuum oven at 120°C overnight. A series of Sn–KS6 composites with different Sn contents was obtained by varying the amount of KS6 present during the precipitation.

Sn was also precipitated without KS6. The metallic Sn obtained as such, and Sn particles from a commercial source (Aldrich, −325 mesh) were used in several Sn–KS6 mechanical mixtures to compare with the electrochemical performance of the Sn–KS6 composites.

2.2. Dispersion of SnO on synthetic graphite KS6

In this case, a 0.05 M LiOH solution was used to precipitate Sn^{2+} as $Sn(OH)_2$ in the presence of suspending KS6 particles. The rate of hydrolysis was carefully controlled to obtain a uniform dispersion of $Sn(OH)_2$ in the carbon host. The solid phase recovered from filtration after copious washing with distilled water was dried in vacuum at 180°C overnight. The amount of KS6 present during the precipitation was varied to obtain a series of SnO-modified graphites. $Sn(OH)_2$ was also precipitated without KS6 to provide as the source of SnO for a series of mechanical mixtures of SnO and KS6 used in the comparison experiments.

2.2.1. Electrochemical tests

A 1-methyl-2-pyrrolidon (NMP) slurry of 80 wt.% of the Sn- or SnO-based anode material and 20 wt.% of polyvinylidene fluoride (PVDF) was used to coat 20-μm-thick copper discs to a mass loading of about 4–5 mg/cm^2 (after drying at 100°C and compaction at 2.0×10^6 Pa). Each coated electrode was assembled into a test cell using a Li counter electrode, a microporous polypropylene separator, and an electrolyte of 1 M $LiPF_6$ solution in a 50:50 (v/v) mixture of ethylene carbonate (EC) and diethyl carbonate (DEC). The assembly was carried out in an Ar-filled glove box with less than 1 ppm each of oxygen and moisture. The cells were charged and discharged at 25°C between 0 and 2 V at a constant current density of 0.4 mA/cm^2 (approximating the C/6 rate) on a Maccor Series 2000 battery tester.

2.2.2. Materials characterisations

The tin contents in the composites were determined by inductively coupled plasma (ICP) spectroscopy using digestions of the composites in a mixture of HCl and HNO_3 (1 M each). Powder X-ray diffractometry using a CuK_α source and scanning electron microscopy were used to examine the composite structure and morphology, respectively.

3. Results and discussion

3.1. The Sn–KS6 series

Fig. 1 shows the typical powder X-ray pattern of a Sn–KS6 composite. The twin diffraction peaks at $2\theta = 30–32°$ and at $2\theta = 43–45°$ are characteristic of metallic Sn [12], and the graphite host is represented by the prominent (002) diffraction at 26.3°. There was no significant reduction in the intensity of the carbon diffraction peak, neither was any peak broadening observed. The formation of the composites, therefore, has not caused any changes to the graphite structure, in particular the d_{002} interlayer spacing. The composites can be described as an intimate mixture of graphite and metallic Sn with the latter visible mostly as tiny white specs among a sea of graphite flakes when being examined by scanning electron microscopy (Fig. 2).

Several important performance indicators of the Sn-KS6 composites are given in Table 1.

In the table, $R_{15/1}$ is the ratio of the specific capacity in the 15th cycle relative to the 1st, and is used as a first indication of material cyclability. It is obvious from Fig. 3(a) that addition of Sn has increased the specific capacity. The increase varies linearly with the tin content indicating that the rule of additivity applies, and that the two active components are practically working independently of each other. The irreversible capacity loss of the pristine carbon is higher than usual primarily because of the large specific surface area of KS6 [13]. Some of the irreversibilities could also have been caused by an unoptimised cell design. Addition of Sn increases the irreversible capacity loss by about 40–70 mA h/g in the first cycle and also reduces material cyclability. From the trends in Fig. 3(b), these

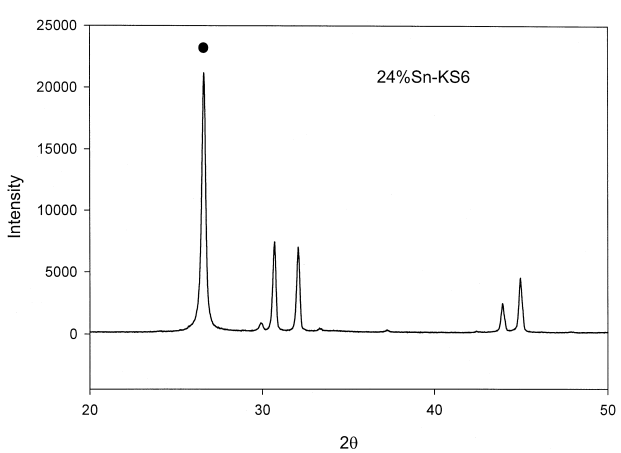

Fig. 1. XRD pattern of 24 wt.% Sn–KS6 composite.

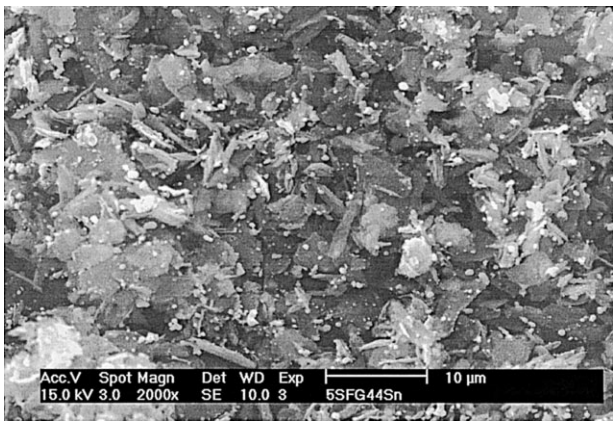

Fig. 2. SEM photo of 24 wt.% Sn–KS6 composite.

effects are also linearly dependent on the Sn content. If not for the deteriorated cyclability, the moderate increase in the first-cycle capacity loss is a small price to pay for the large increase in specific capacity.

As Sn was not present initially as an oxide precursor, the first-cycle irreversible capacity is likely related to electrolyte decomposition and passive film formation on the Sn surface similar to the solid electrolyte interface (SEI) formation on a carbonaceous surface. Electrochemical impedance measurements [14] and FTIR investigations [15] have confirmed the presence of passivating layers on the surface of SnO and related compounds and that the film formation process is consumptive of Li^+ ions. These passivating films are not effective SEI because the large volume change in lithium insertion and extraction reactions always exposes new surfaces for further reactions.

The Sn–KS6 composites still suffer from noticeable capacity fades over cycling, although the extent of which is small compared to some of the previous efforts [7,8]. This is taken to indicate that Sn is highly dispersed in KS6 (the linearity between specific capacity and Sn content suggests that the dispersion of Sn is almost equal in all samples), and the aggregation of small Sn particles (with ensuing application problems) are hindered by the intervening carbonaceous phase whose good electrical conductivity allows most of the particles remain electrically connected. The ductility of carbon also serves to buffer the internal stress caused by the volume changes in lithium insertion and extraction reactions.

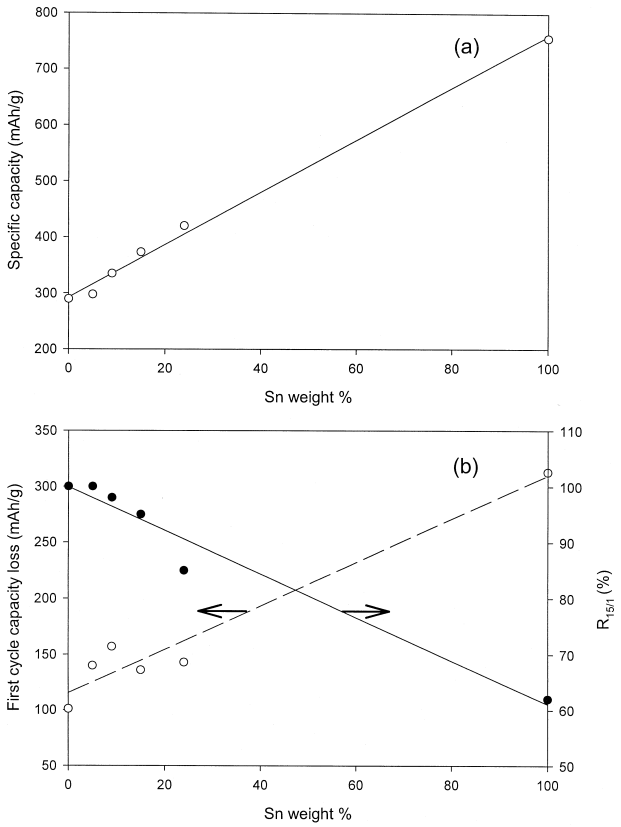

Fig. 3. Specific capacity (a) and first-cycle characteristics (b) of the Sn–KS6 series.

It is definitely of interest to benchmark the performance of the composites against physically mixtures of Sn and KS6 made by conventional means. Comparative experiments were, therefore, carried out, in which KS6 was mechanically mixed with Sn particles prepared from the $NaBH_4$ reduction of Sn^{2+} (typically < 1 μ) or Sn particles from a commercial source (-325 mesh or < 44 μ). The electrochemical performance of the mechanical mixtures in the first cycle is summarized in Table 2 below:

The specific capacity and the irreversible capacity loss of the mechanical mixtures are comparable to that of the KS6–SnO series. Lower material utilization was only found in samples where larger Sn particles (44 μ) were used. Preliminary tests on the cyclability of the mechanical mixtures also result in similar trends, with the larger Sn particles showing more signs of capacity fade. These results indicate that there is no specific interaction between

Table 1
Performance of Sn–KS6 composites

Tin content (wt.%)	0	5	9	15	24	100
Specific capacity (mA h/g active)	290	298	335	373	420	756
1st cycle capacity loss (mA h/g)	101	140	167	136	143	313
1st cycle Coulombic efficiency (%)	55	55	56	64	69	69
$R_{15/1}$	100	100	98	95	85	62

Table 2
Performance of mechanically mixed KS6 and Sn particles

Source of Sn particles	$NaBH_4$ reduction			Commercial		
Tin content (wt.%)	12	19	24	12	20	25
Specific capacity (mA h/g active)	370	390	397	356	330	365
1st cycle capacity loss (mA h/g)	133	130	134	102	109	116
1st cycle Coulombic efficiency (%)	60	67.5	75	62	60	64

Sn and KS6 that can greatly enhance the dispersion of the former beyond what is possible by mechanical means.

3.2. The SnO–KS6 series

More interesting results were obtained from the SnO-modified graphites. The scanning electron micrographs in Fig. 4 show that SnO is uniformly distributed over the surface of KS6. Quite unlike the case of Sn dispersion in KS6, where Sn is detected as identifiable foreign particles on the KS6 surface, the surface of the SnO–KS6 composite is exceedingly homogeneous with the alternating light and shadow areas, indicating more of variations in surface profiles rather than phase heterogeneities. The oxide anions in SnO could have bridged with carbon surface species to result in good spreading between SnO and the graphite. However, SnO is not present as an impervious coating on graphite to interfere with the movement of Li^+ in the intercalation and de-intercalation reactions through the prismatic faces.

From the XRD spectra of Fig. 5, the additional diffraction peaks that appear after the addition of SnO confirms the presence of tin oxides [2,16]. The modified graphites were also found to scatter the X-ray more incoherently, resulting in low diffraction intensities. However, a closer examination of the spectra reveals that the graphite peaks are not shifted and there is no significant peak broadening indicative of substantial alternations of the graphite structure.

The SnO contents of a number of modified graphite anodes as analysed by ICP are given in Table 3. Also shown in the Table are the reversible specific capacities and the ratios of the capacity in the 10th cycle relative to the 1st, $R_{10/1}$, which are used to indicate material endurance to repeated cyclic operations. There is an immediate increase in capacity after SnO addition, but that comes amidst some loss of cyclability. In some cases, the specific capacities of the composites are even larger than the weighted sums of the theoretical capacities of graphite (372 mA h/g) and SnO (875 mA h/g). When the specific capacities of the various samples are plotted against the weight fraction of SnO (Fig. 6), a straight line can be drawn to intercept the capacity axis at 353 mA h/g. As pristine KS6 could only deliver 300 mA h/g experimentally, the increase in specific capacity is attributed to the presence of SnO in KS6, even at very low concentrations. SnO could have facilitated the formation of the SEI, or the formation of a more compact SEI on the graphite surface, as has been suggested for the case of CuO addition to graphite [17]. The linear trend also projects a specific capacity of 1080 mA h/g for the pure SnO, which translates into an uptake of about 5.4 Li atoms per Sn atom. The projection is much higher than the commonly observed intercalation level of 4.4 Li atoms per Sn atom. It seemingly suggests the existence of synergistic interaction between graphite and SnO and that the capacity of the composite is not a simple weighted sum of the capacities of the individual components.

The first two-cycle charging (Li intercalation) and discharging (Li de-intercalation) curves are shown in Fig. 7. The difference in voltage profiles between pristine and SnO-modified graphites is immediately apparent. Although all samples have shown some irreversible capacity losses

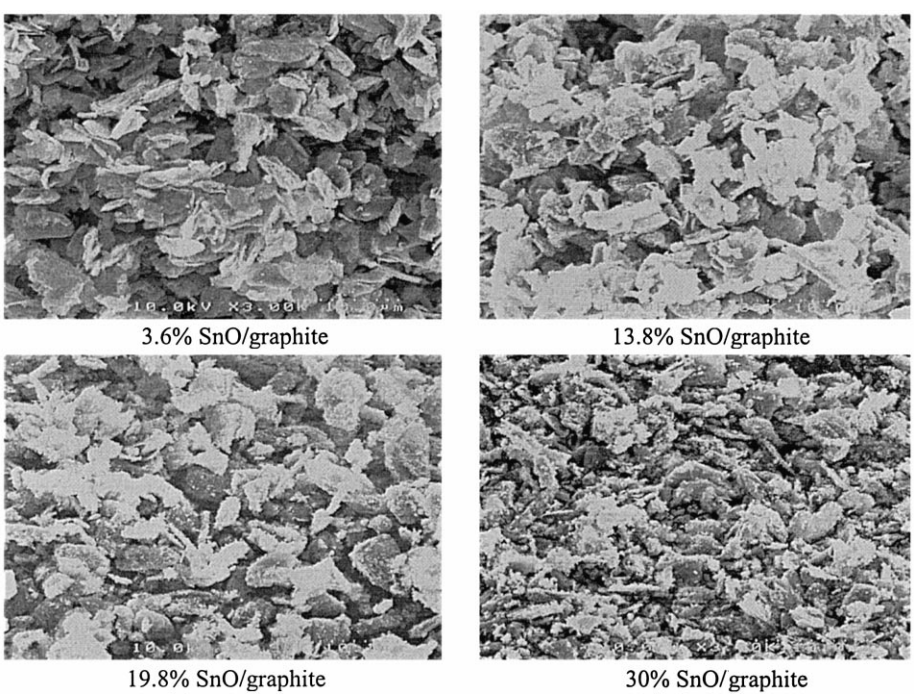

Fig. 4. SEM photos of SnO–KS6 composites.

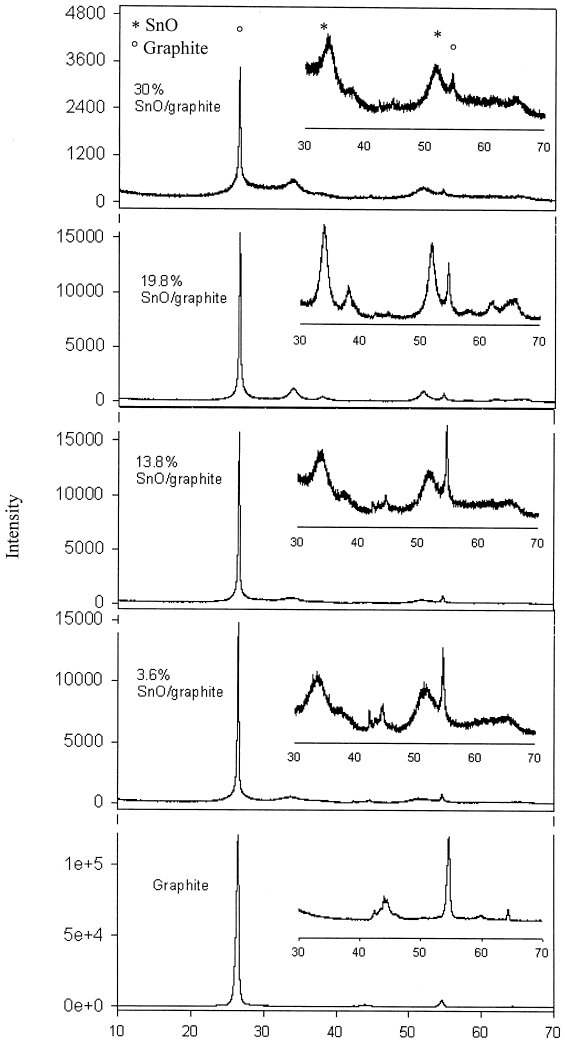

Fig. 5. XRD patterns of SnO–KS6 composites.

in their first cycles, the extent of the loss is more severe after the addition of SnO, even at a level as low as 3.6 wt.% of SnO. The first cycle charging curve for graphite is marked by a short plateau at 0.8 V characteristic of the start of SEI formation, and the extended flat voltage profile near 0 V indicative of staged insertions in the graphene layers. For SnO-modified graphites, there are discernible additional potential plateaus above 1.0 V that are not apparent in subsequent cycles. The lengths of these plateaus are approximately proportional to the SnO contents in the composites.

Table 3
Electrochemical performances of various SnO-graphite composite anodes

SnO content (wt.%)	0	3.6	13.8	19.8	30
Specific capacity (mA h/g active)	300	380	450	500	570
1st cycle capacity loss (mA h/g)	116	321	412	443	450
1st cycle Coulombic efficiency (%)	57	54	58	52	55
$R_{10/1}$	100	95	96	80	80

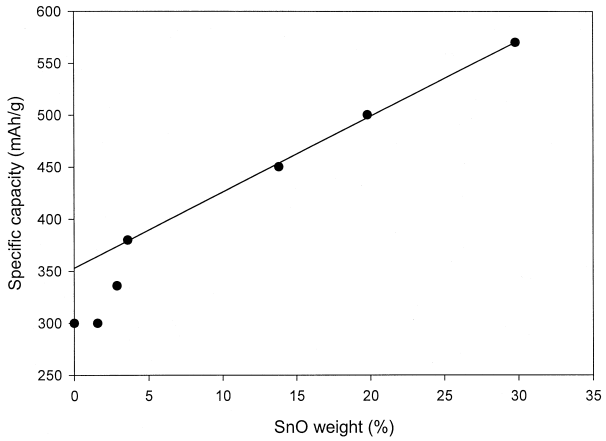

Fig. 6. Specific capacity of SnO-modified KS6 as a function of SnO loading.

The cyclability of a typical SnO-modified graphite (13.8 wt.%) relative to pristine graphite and pristine SnO was determined at two different current densities (Fig. 8). The last sample displays the characteristic discharge behaviour of pure SnO: high initial specific capacity that is undermined by an equally high fade rate (indication that the Li_2O phase has not provided adequate protection). For pristine KS6, the specific capacity is virtually unchanged in 30 cycles at the two current densities tested. The SnO-modified graphite has a higher specific capacity relative to pristine graphite due to the presence of SnO and displays the normal material behaviour of reduced capacity

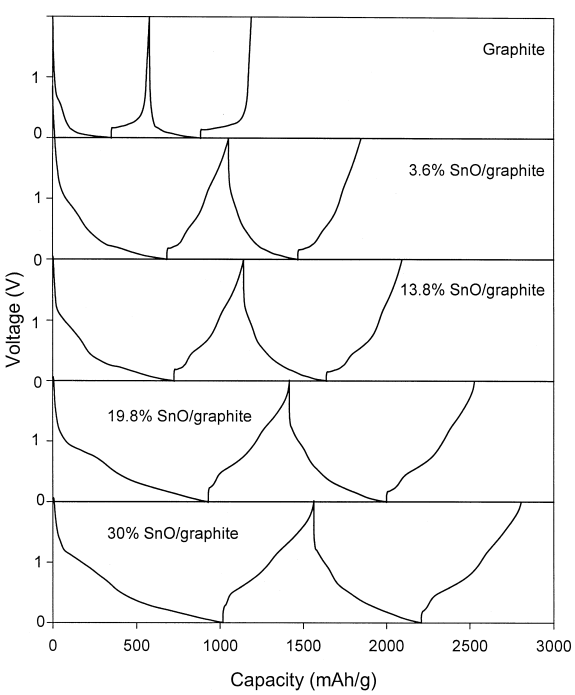

Fig. 7. The first two-cycle charging and discharging curves of various SnO–KS6 composites.

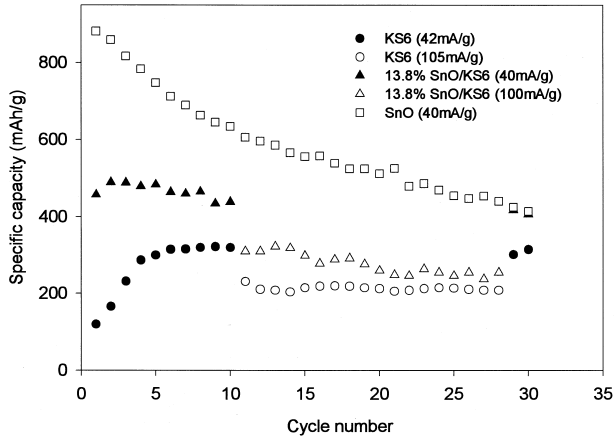

Fig. 8. Cyclability of the SnO–KS6 series at different current densities.

at a higher current density. Although there is some slight capacity fade over the period of 30 cycles, the extent of the fade is significantly lower than that of bulk SnO. Increase in current density appears to accelerate the fade, but the overall result is still a substantial improvement over pristine SnO.

Mechanical mixtures of SnO and KS6 of similar overall compositions were also prepared. The increase in the capacity of KS6 was not replicated by these samples and they had much poorer cycling performance relative to the chemically prepared composites. The preparative procedure, therefore, has succeeded in producing small, localized domains of SnO, which alleviate many of the mechanical property-linked application deficiencies of the bulk SnO system in reversible Li ion storage.

4. Conclusions

The utilisation of Sn and SnO as Li ion storage compounds can be greatly improved by dispersing them on a large surface-area substrate. This allows diminution of the active materials to reduce the overall impact of their mechanical disintegration, which is mostly responsible for the observed capacity fading. The substrate should preferably be electronically conductive to ensure that the particles remain electrically connected, regardless of whether particle pulverisation has taken place. Additionally, the substrate can be an active lithium-storage compound to add to the overall capacity of the composite material. We have noticed that synthetic graphite of adequately large surface area (e.g. KS6) has satisfied categorically many of these aforesaid attributes. Sn–KS6 and SnO–KS6 composites have been prepared that perform much better than when these Sn-based materials were used singly without the graphite support. The preparative procedures still need to be further refined to lower the irreversibility capacity loss and to increase long-term cyclability. An outstanding dilemma lies with the use of large surface-area carbon for dispersion, which unfortunately brings in large irreversible capacity losses. An alternative view is to use the Sn compounds sparingly as anode additives to improve the specific capacity of graphite. The experimental results presented here clearly indicate the feasibility of such an approach.

References

[1] Y. Idota, A. Matsufuji, Y. Maekawa, T. Miyasaki, Science 276 (1997) 1395.
[2] I.A. Courtney, J.R. Dahn, J. Electrochem. Soc. 144 (1997) 2045.
[3] W. Liu, X. Huang, Z. Wang, H. Li, L. Chen, J. Electrochem. Soc. 145 (1998) 49.
[4] O. Mao, R.L. Turner, I.A. Courtney, B.D. Fredericksen, M.I. Buckett, L.J. Krause, J.R. Dahn, Electrochem. Solid-State Lett. 2 (1999) 3.
[5] G.R. Goward, F. Leroux, W.P. Power, G. Ouvrard, W. Dmowski, T. Egami, L.F. Nazrar, Electrochem. Solid-State Lett. 2 (1999) 367.
[6] I.A. Courtney, W.R. McKinnon, J.R. Dahn, J. Electrochem. Soc. 146 (1999) 59.
[7] A.H. Whitehead, J.M. Elliot, J.R. Owen, J. Power Sources 81–82 (1999) 33.
[8] H. Li, X. Huang, L. Chen, J. Power Sources 81–82 (1999) 335.
[9] J.O. Besenhard, J. Yang, M. Winter, J. Power Sources 68 (1997) 87.
[10] J. Wolfenstein, D. Foster, J. Read, W.K. Behl, W. Leuecke, in: Abstract 263, The 1999 Joint International Meeting Abstracts, Honolulu, HI, October 17–22, 1999.
[11] P. Limthongkul, Y.M. Chiang, in: Abstract 330, The 1999 Joint International Meeting Abstracts, Honolulu, HI, October 17–22, 1999.
[12] T. Brousse, R. Retoux, U. Herterich, D.M. Schleich, J. Electrochem. Soc. 145 (1998) 1.
[13] M. Winter, P. Novak, A. Mannier, J. Electrochem. Soc. 145 (1998) 428.
[14] H. Li, X. Huang, L. Chen, J. Power Sources 81–82 (1999) 340.
[15] J. Li, H. Li, Z. Wang, X. Wang, L. Chen, J. Power Sources 81–82 (1999) 346.
[16] I.A. Courtney, J.R. Dahn, J. Electrochem. Soc. 144 (1997) 2943.
[17] J. Wei, J.Y. Lee, in: S. Surampudi, R.A. Marsh (Eds.), Lithium Batteries, The Electrochemical Society Proceedings Series, Pennington, NJ, 1999, p. 51, PV98-16.